

The Liquid-Gas Phase Transitions in a Multicomponent Nuclear System with Coulomb and Surface Effects

S.J. Lee* and A.Z. Mekjian

Department of Physics and Astronomy, Rutgers University, Piscataway, New Jersey 08855

The liquid-gas phase transition is studied in a multi-component nuclear system using a local Skyrme interaction with Coulomb and surface effects. Some features are qualitatively the same as the results of Müller and Serot which uses relativistic mean field without Coulomb and surface effects. Surface tension brings the coexistence binodal surface to lower pressure. The Coulomb interaction makes the binodal surface smaller and cause another pair of binodal points at low pressure and large proton fraction with less protons in liquid phase and more protons in gas phase.

PACS no.: 24.10.Pa, 21.65.+f, 05.70.-a, 64.10.+h

I. INTRODUCTION

The liquid-gas phase transition in nuclei was first studied using a Skyrme interaction and focussed mostly on one component systems of just nucleons even though expressions were developed for two component systems of protons and neutrons [1]. The phase transition aspects are considerably easier to study in one component systems rather than two, where for example one has to deal with separate proton and neutron chemical potentials for charge and nucleon number conservation. Initial fragmentation models also mostly dealt with one component systems. Such fragmentation studies gave the first evidence for the liquid-gas phase transition in nuclear systems [2,3]. Since then, the liquid-gas phase transition has been extensively studied experimentally and theoretically. Several reviews exist on this topic [4–6].

Because of the two component nature of real nuclear systems, an analysis of liquid-gas phase transition in these systems is important. Some preliminary results were reported in Ref. [1], and a very detailed study was done by Müller and Serot [7] who used a relativistic mean field model to develop the main thermodynamic properties of asymmetric nuclear matter. One interesting new aspect of two component system compared to one component system is that the phase transition is a second order transition in their approach. The importance of the number of components on the order of the transition was pointed out by Glendenning [8]. Another interesting aspect of two component systems is the possibility of having different proton–neutron ratios in the liquid and gas phases because of the symmetry energy. The study of nuclear systems with arbitrary proton–neutron ratios is important for radioactive beam experiments and in astrophysical situations as in neutron stars. Because of the extra degree of freedom associated with varying proton fraction y in the two phases, the phase diagram has a higher dimensionality and now becomes a surface in pressure P , temperature T , and proton fraction y or nucleon density ρ . For one component systems the phase diagram is represented as a binodal curve of P versus density ρ or volume V , whose end points at fixed T give the liquid and gas densities. The Maxwell pressure versus T in one component systems is a line that terminate at the critical temperature T_c . For two component systems, the binodal surface associated with phase coexistence in (P, T, y) now contains a line of critical points for different values of y , a line for the Maxwell pressure versus T for a symmetric system at $y = 0.5$ which has a the smallest P and is the same as for a one component system, and a line of maximal asymmetry. At fixed T , P versus y of binodal points form loops and $(dy/dP)_T = 0$ gives a point of maximal asymmetry or smallest proton ratio on the binodal surface.

In this paper we extend the initial study of Ref. [1] using Skyrme interaction in a similar way as done in Ref. [7]. Some features are qualitatively the same as in Ref. [7], but quantitatively differ because of the different interaction. Our equation of state based on the Skyrme interaction with Coulomb and surface effects has some feature also not present in Ref. [7] which will also be discussed. According to the results of Ref. [7] which has no Coulomb interaction, the liquid phase has higher proton fraction than the gas phase of mixed phases in the coexistent state. A real nucleus has less protons than neutrons due to Coulomb interaction. For a given $A = N + Z$ stability is determined by Coulomb and symmetry energy effects. Since a stable finite nucleus has zero internal pressure while the gas phase having positive pressure [9], we also need to consider surface effects. In this paper we consider the effects of Coulomb interaction and surface tension by considering uniform spherical finite nuclear system.

In Section II, the main equations for the thermodynamic properties of hot nuclear matter in mean field theory are developed as a function of density ρ , temperature T , and proton fraction y or neutron fraction $(1 - y)$. These include the pressure and chemical potentials, both neutron μ_n and proton μ_p where phase equilibrium requires equality of the proton chemical potential between the two phases and similarly equality of the neutron chemical potentials at a given temperature and P . At fixed T and P , ρ and y are not independent and we use this connection to simplify

the analysis. Section III contains the results of calculations performed using the equations developed in Section II. Conclusions are given in Section IV.

II. PHASE TRANSITION IN MEAN FIELD THEORY

For phase transition we look at the pressure P and chemical potentials μ_q for each component of multi-component system (neutron and proton for example) as functions of temperature T and the densities ρ_q of the constituents. These quantities can be obtained once we know the total energy functional E as a function of the densities ρ_q at a given temperature T .

At a given temperature $T = 1/\beta$, the constituents are distributed in phase space according to the Wigner function f as

$$f(\vec{r}, \vec{p}) = \sum_q f_q(\vec{r}, \vec{p}), \quad f_q(\vec{r}, \vec{p}) = \frac{\gamma}{h^3} \tilde{f}_q(\vec{r}, \vec{p}) = \frac{\gamma}{h^3} \frac{1}{e^{\beta(\epsilon_q - \mu_q)} + 1} \quad (1)$$

where the spin degeneracy $\gamma = 2$ and ϵ_q and μ_q are the single particle energy and the chemical potential of particle type q . Then the particle density ρ becomes

$$\rho(\vec{r}) = \sum_q \rho_q(\vec{r}), \quad \rho_q(\vec{r}) = \int d^3p f_q(\vec{r}, \vec{p}), \quad (2)$$

$$A = \sum_q N_q = \int d^3r \rho(\vec{r}), \quad N_q = \int d^3r \rho_q(\vec{r}) = \int d^3r \int d^3p f_q(\vec{r}, \vec{p}) \quad (3)$$

and the total energy is

$$E = \int d^3r \mathcal{E}(\vec{r}) = \int d^3r \int d^3p \frac{p^2}{2m} f(\vec{r}, \vec{p}) + \int d^3r U(\vec{r}) = \int d^3r [\mathcal{E}_K(\vec{r}) + U(\vec{r})] \quad (4)$$

with the potential energy density $U(\vec{r})$ and the kinetic energy density $\mathcal{E}_K(\vec{r})$. These, in turn, give self-consistent equations for μ_q (or p_{Fq}) in a mean field theory for fixed T and N_q ,

$$\epsilon_q = \frac{\delta E}{\delta f_q} = \frac{\delta \mathcal{E}(\vec{r})}{\delta f_q(\vec{r}, \vec{p})} = \frac{p^2}{2m} + \frac{\delta U}{\delta f_q} = \frac{p^2}{2m} + u_q(\vec{r}, \vec{p}) \quad (5)$$

$$\mu_q = \epsilon_q|_{p=p_{Fq}} = \frac{p_{Fq}^2}{2m} + u_q(\vec{r}, \vec{p}_{Fq}) \quad (6)$$

where we define p_{Fq} in Eq.(6) and consider it as an effective Fermi momentum at T of particle q , which is the momentum associated with the chemical potential, and $u_q = \frac{\delta U}{\delta f_q}$ is the single particle potential of particle q which may be momentum dependent in general.

The pressure P can be defined dynamically from the total momentum conservation law, $\frac{d}{dt} [\int d^3r \int d^3p \vec{p} f] = - \int d^3r \vec{\nabla}_r \cdot \overset{\leftrightarrow}{\Pi} = 0$, using the Vlasov equation [10]

$$\frac{\partial f_q}{\partial t} + (\vec{\nabla}_p \epsilon_q) \cdot (\vec{\nabla}_r f_q) - (\vec{\nabla}_r \epsilon_q) \cdot (\vec{\nabla}_p f_q) = 0 \quad (7)$$

or more generally from hydrodynamic consideration of TDHF in phase space [11]

$$\begin{aligned} \vec{\nabla}_r \cdot \overset{\leftrightarrow}{\Pi} &= -\frac{d}{dt} \left[\int d^3p \vec{p} \sum_q f_q(\vec{r}, \vec{p}) \right] = -\sum_q \int d^3p \vec{p} \left(\frac{\partial f_q}{\partial t} \right) \\ &= \sum_q \int d^3p \vec{p} \cdot \vec{\nabla}_r \left[(\vec{\nabla}_p \epsilon_q) f_q \right] + \sum_q \int d^3p \vec{p} \cdot (\vec{\nabla}_r \epsilon_q) f_q \end{aligned} \quad (8)$$

where \hat{p} is the unit vector in the direction of \vec{p} . Using $(\vec{\nabla}_r \epsilon_q) f_q = \vec{\nabla}_r (\epsilon_q f_q) - \epsilon_q \vec{\nabla}_r f_q = \vec{\nabla}_r (\epsilon_q f_q) - \vec{\nabla}_r \mathcal{E}$, the dynamical pressure tensor Π_{ij} becomes

$$\begin{aligned}
\Pi_{ij} &= \sum_q \int d^3p p_i (\nabla_p^j \epsilon_q) f_q + \delta_{ij} \left[\int d^3p \sum_q \epsilon_q f_q - \mathcal{E} \right] \\
&= \sum_q \int d^3p p_i \nabla_p^j \left(\frac{\delta \mathcal{E}}{\delta f_q} \right) f_q + \delta_{ij} \left[\sum_q \int d^3p \left(\frac{\delta \mathcal{E}}{\delta f_q} \right) f_q - \mathcal{E} \right] \\
&= \sum_q \int d^3p p_i \left[\frac{p_j}{m} + \nabla_p^j \left(\frac{\delta U}{\delta f_q} \right) \right] f_q + \delta_{ij} \left[\sum_q \int d^3p \left(\frac{\delta U}{\delta f_q} \right) f_q - U \right]
\end{aligned} \tag{9}$$

For a momentum independent potential, this becomes

$$\Pi_{ij} = \sum_q \int d^3p \frac{p_i p_j}{m} f_q + \delta_{ij} \left[\sum_q \left(\frac{\delta U}{\delta \rho_q} \right) \rho_q - U \right] = \int d^3p \sum_q \frac{p_i p_j}{m} f_q + \delta_{ij} \sum_q \rho_q^2 \frac{\delta(U/\rho_q)}{\delta \rho_q} \tag{10}$$

The diagonal elements are

$$P = \Pi_{ii} = \sum_q \int d^3p \frac{p_i^2}{m} f_q + \sum_q \frac{\delta U}{\delta \rho_q} \rho_q - U = P_K + \sum_q u_q \rho_q - U = P_K + P_P \tag{11}$$

where $P_K = \int d^3p \frac{p^2}{m} f$ and $P_P = \sum_q u_q \rho_q - U$ are the kinetic pressure and interaction (potential) pressure respectively. In equilibrium P can also be obtained by minimizing the total energy as a function of volume holding the number of particles fixed:

$$P = \Pi_{ii} = - \frac{d(E/A)}{dV} = \rho^2 \frac{d(\mathcal{E}/\rho)}{d\rho} \tag{12}$$

for a single component uniform system.

From the distribution \tilde{f}_q of Eq.(1), the entropy S can be obtained as,

$$S = \sum_q S_q = \int d^3r \mathcal{S} = \int d^3r \sum_q \mathcal{S}_q, \tag{13}$$

$$\begin{aligned}
\mathcal{S}_q &= - \frac{\gamma}{h^3} \int d^3p \left[\tilde{f}_q \ln \tilde{f}_q + (1 - \tilde{f}_q) \ln(1 - \tilde{f}_q) \right] \\
&= \frac{\gamma}{h^3} \int d^3p \frac{1}{3} \vec{p} \cdot (\vec{\nabla}_p \tilde{f}_q) \ln \left[\frac{\tilde{f}_q}{1 - \tilde{f}_q} \right] \\
&= \frac{\gamma}{h^3} \int d^3p \frac{1}{3} \vec{p} \cdot (\vec{\nabla}_p \tilde{f}_q) \beta (\mu_q - \epsilon_q)
\end{aligned} \tag{14}$$

using $\vec{\nabla}_p \cdot (\vec{p}g) = 3g + \vec{p} \cdot \vec{\nabla}_p g$. The \mathcal{S}_q becomes, by partial integration [12],

$$\begin{aligned}
\mathcal{S}_q &= \beta \int d^3p \frac{1}{3} \vec{p} \cdot \vec{\nabla}_p [(\mu_q - \epsilon_q) f_q] - \beta \int d^3p \frac{1}{3} \vec{p} \cdot \vec{\nabla}_p (\mu_q - \epsilon_q) f_q \\
&= \beta \int d^3p (\epsilon_q - \mu_q) f_q + \beta \int d^3p \frac{\vec{p} \cdot \vec{\nabla}_p \epsilon_q}{3} f_q \\
&= \beta \int d^3p \epsilon_q f_q + \beta \int d^3p \frac{\vec{p} \cdot \vec{\nabla}_p \epsilon_q}{3} f_q - \beta \mu_q \int d^3p f_q
\end{aligned} \tag{15}$$

In equilibrium thermodynamics, the thermodynamic grand potential Ω , the Helmholtz free energy F , and the Gibb's free energy G are

$$\Omega = - \int d^3r P = - \frac{1}{\beta} \ln \text{Tre}^{-\beta(\hat{H} - \sum_q \mu_q \hat{N}_q)} = F - G = E - TS - \sum_q \mu_q N_q, \tag{16}$$

$$F = \int d^3r \mathcal{F} = - \frac{1}{\beta} \ln \text{Tre}^{-\beta \hat{H}} = E - TS = T \int E d\beta, \tag{17}$$

$$G = \int d^3r \mathcal{G} = \frac{1}{\beta} \ln \text{Tre}^{\beta \sum_q \mu_q \hat{N}} = \sum_q \mu_q N_q = \int d^3r \sum_q \mu_q \rho_q \tag{18}$$

Comparing Eq.(15) with Eq.(9) for diagonal elements using $p_i \nabla_p^i = \frac{1}{3} \vec{p} \cdot \vec{\nabla}_p$ (isotropic condition in momentum, $p_i^2 = \frac{1}{3} p^2$),

$$TS = \mathcal{E} + P - \sum_q \mu_q \rho_q = \mathcal{E} - \mathcal{F} = \mathcal{E}_K + P_K - \sum_q (\mu_q - u_q) \rho_q, \quad (19)$$

$$\mathcal{F} = \sum_q \mu_q \rho_q - P = \sum_q (\mu_q - u_q) \rho_q - P_K + U, \quad (20)$$

$$\mathcal{G} = \sum_q \mathcal{G}_q = \sum_q \mu_q \rho_q \quad (21)$$

The entropy can also be found from $dQ = TdS = CdT$;

$$\Delta S = \int \frac{dQ}{T} = \int \frac{CdT}{T} = \int \frac{1}{T} \frac{dE}{dT} dT = \int \beta \frac{dE}{d\beta} d\beta = \beta E - \int E d\beta = \beta (E - F) \quad (22)$$

The pressure and the chemical potential are also related to the free energy F as

$$P = - \left. \frac{\partial F}{\partial V} \right|_{T,A} = - \left. \frac{\partial \Omega}{\partial V} \right|_{T,A}, \quad (23)$$

$$\mu = \left. \frac{\partial F}{\partial A} \right|_{T,V} \quad (24)$$

The specific heat capacity is given by from the entropy per particle, \mathcal{S}/ρ ,

$$c_P = T \left(\frac{\partial \mathcal{S}/\rho}{\partial T} \right)_P \quad \text{or} \quad c_V = T \left(\frac{\partial \mathcal{S}/\rho}{\partial T} \right)_V \quad (25)$$

To study the caloric curve or the specific heat we look at the enegy per particle \mathcal{E}/ρ and the entropy per particle \mathcal{S}/ρ .

For multi-phase multi-component system, the phase transition of each component can occur at different conditions such as temperature or pressure. However in general we can treat all the different possible combinations of phases of each component in the multi-component system as different phases of the system. (As an example suppose we have a system of particles of type p and particles of type n, each having a liquid-gas phase transition but at different temperatures. Then the system can be in one of the following four phases; a phase of liquid p and liquid n, a phase of liquid p and gas n, a phase of gas p and liquid n, or a phase of gas p and gas n.) Then, to separate each phase of the multi-component system, we can use the volume fraction λ_i of i -phase of total volume V which depends on T ,

$$\lambda_i = V_i/V \quad \text{with} \quad \sum_i \lambda_i = 1, \quad (26)$$

$$\rho_q = \sum_i \lambda_i \rho_q^i, \quad (27)$$

$$\mathcal{O}(\rho_q, T) = \sum_i \lambda_i \mathcal{O}(T, \rho_q^i) \quad (28)$$

where \mathcal{O} is any obserbable per unit volume. Within the spinodal instability region, there is no equilibrated phase. Two or multi phases can coexist when the pressure P and each chemical potential μ_q are all the same among these phases, i.e.,

$$P_i = P_j, \quad (29)$$

$$\mu_q^i = \mu_q^j \quad (30)$$

with different values of ρ_q^i and ρ_q^j for all i and j . At the critical point

$$\frac{\partial P}{\partial \rho_q} = \frac{\partial^2 P}{\partial \rho_q^2} = 0, \quad (31)$$

$$\frac{\partial \mu_q}{\partial \rho_q} = \frac{\partial^2 \mu_q}{\partial \rho_q^2} = 0 \quad (32)$$

Spinodal instability occurs when $\frac{\partial P}{\partial \rho_q}$ is negative.

Once the potential energy U in Eq.(4) is known, then the possibility of a phase transition of the system can be studied using Eqs.(1) – (25). The potential energy U determines ϵ_q and μ_q and the potential energy part of E and P . Then for fixed T and N_q , the Wigner function f and p_{Fq} are determined and thus the kinetic terms of E , μ_q , and P . Using these results, the entropy S and c_P can be determined. Relativistic mean field theory is used for the interaction in Ref. [7]. The role of the Coulomb interaction and surface energy or the finite size effect of a nucleus are neglected in Ref. [7] but will be included in the approach developed here. Their result shows that the neutron evaporates first as the energy of the system increases leaving more charge concentrated in liquid phase. In this approach the coupled equations of nucleon and mesons lead to a highly nonlinear system and thus the equation of state can be obtained only through self-consistent iterative way. These problems may be simplified by using a nonrelativistic zero-range Skyrme interaction of

$$v_{12} = t_0(1 + x_0 P^\sigma)\delta(\vec{r}_1 - \vec{r}_2) + \frac{t_3}{6}(1 + x_3 P^\sigma)\rho^\alpha\left(\frac{\vec{r}_1 + \vec{r}_2}{2}\right)\delta(\vec{r}_1 - \vec{r}_2) \quad (33)$$

For a nuclear system of proton (ρ_p) and neutron (ρ_n), this gives the local potential energy density as

$$U(\rho_q) = \frac{t_0}{2}\left(1 + \frac{x_0}{2}\right)\rho^2 - \frac{t_0}{2}\left(\frac{1}{2} + x_0\right)\sum_q \rho_q^2 + \frac{t_3}{12}\left(1 + \frac{x_3}{2}\right)\rho^{\alpha+2} - \frac{t_3}{12}\left(\frac{1}{2} + x_3\right)\rho^\alpha\sum_q \rho_q^2 + C\rho^\beta\rho_p^2 + C_s\rho^\eta \quad (34)$$

Here $C\rho^\beta = \frac{4\pi}{5}e^2R^2$ and $C_s\rho^\eta = \frac{4\pi R^2\sigma(\rho)}{V} = \frac{(4\pi r_0^2\sigma)}{V^{1/3}}\rho^{2/3}$ when we approximate the Coulomb and surface effects as coming from a finite uniform sphere of radius $R = r_0A^{1/3}$ with total charge Z ($U_C = \frac{3}{5}\frac{e^2Z^2}{RV}$). The typical values for the force parameters are given in Table I. For a symmetric nucleus, $N = Z$, $\rho_q = \rho/2$, and thus

$$U(\rho) = \frac{3}{8}t_0\rho^2 + \frac{3}{48}t_3\rho^{\alpha+2} + C\rho^\beta\rho_p^2 + C_s\rho^\eta \quad (35)$$

This potential energy determines the interaction dependent terms of \mathcal{E} , P , ϵ_q , and μ_q which depend on densities without explicit T dependence.

For a momentum independent potential energy as in Eq.(34), $\epsilon_q - \mu_q = (p^2 - p_{Fq}^2)/(2m)$ is independent of the potential and

$$f_q(\vec{r}, \vec{p}) = \frac{\gamma}{h^3}\tilde{f}_q(\vec{r}, \vec{p}), \quad \tilde{f}_q(\vec{r}, \vec{p}) = \frac{1}{e^{\beta(p^2 - p_{Fq}^2)/(2m)} + 1} \quad (36)$$

Thus we can evaluate the kinetic terms in \mathcal{E} , P , and μ_q which are functions of T and p_{Fq} . Defining Fermi integral $F_\alpha(\eta)$

$$F_\alpha(\eta_q) = \int_0^\infty \frac{x^\alpha}{1 + e^{x - \eta_q}} dx = \left(\frac{\lambda^2}{4\pi\hbar^2}\right)^{\alpha+1} \int_0^\infty \frac{2p^{2\alpha+1} dp}{1 + e^{\beta p^2/2m - \eta_q}}, \quad (37)$$

$$\eta_q = \beta(\mu_q - u_q) = \beta p_{Fq}^2/(2m) = p_{Fq}^2/(2mT) = \ln z_q, \quad (38)$$

$$\lambda = \sqrt{2\pi\hbar^2/mT} \quad (39)$$

we can write, for $f(\vec{r}, \vec{p}) = f(\vec{r}, p)$,

$$\rho_q = \int d^3p f_q(\vec{r}, \vec{p}) = \frac{\gamma}{h^3} \int d^3p \frac{1}{e^{\beta(p^2 - p_{Fq}^2)/(2m)} + 1} = \lambda^{-3} \frac{2\gamma}{\sqrt{\pi}} F_{1/2}(\eta_q), \quad (40)$$

$$\epsilon_{Fq} \equiv \frac{\hbar^2}{2m} \left(\frac{6\pi^2}{\gamma} \rho_q\right)^{2/3}, \quad (41)$$

$$\begin{aligned} \mathcal{E}_{Kq} &= \frac{3}{2}P_{Kq} = \int d^3p \frac{p^2}{2m} f_q(\vec{r}, \vec{p}) = \frac{\gamma}{h^3} \int d^3p \frac{p^2}{2m} \frac{1}{e^{\beta(p^2 - p_{Fq}^2)/(2m)} + 1} \\ &= \frac{4\gamma\hbar^2\sqrt{\pi}}{m} \lambda^{-5} F_{3/2}(\eta_q) = \frac{1}{\beta} \frac{2\gamma}{\sqrt{\pi}} \lambda^{-3} F_{3/2}(\eta_q) \end{aligned} \quad (42)$$

Here ϵ_{Fq} is the chemical potential at absolute zero or Fermi energy and p_{Fq} is the effective Fermi momentum at T . The particle number $N_q = \int d^3r \rho(\vec{r})$ determines the effective Fermi momentum $p_{Fq}(\vec{r})$ or η_q at T , in terms of density $\rho_q(\vec{r})$,

$$\eta_q(\rho_q, T) = \beta(\mu_q - u_q) = \beta \frac{p_{Fq}^2}{2m} = F_{1/2}^{-1} \left(\frac{\sqrt{\pi}}{2\gamma} \lambda^3 \rho_q \right) \quad (43)$$

For multi(two)-component systems with potential energy given by Eq.(34), for a given ρ_q (or p_{Fq}) and T ,

$$\begin{aligned} \mu_q(\rho_q, T) &= T\eta_q(\rho_q, T) \\ &+ t_0 \left(1 + \frac{x_0}{2}\right) \rho + \frac{t_3}{12} \left(1 + \frac{x_3}{2}\right) (\alpha + 2) \rho^{\alpha+1} - \frac{t_3}{12} \left(\frac{1}{2} + x_3\right) \alpha \rho^{\alpha+1} \\ &- t_0 \left(\frac{1}{2} + x_0\right) \rho_q + \frac{t_3}{12} \left(\frac{1}{2} + x_3\right) (\alpha - 1) 2 \rho^\alpha \rho_q - \frac{t_3}{12} \left(\frac{1}{2} + x_3\right) 2 \alpha \rho^{\alpha-1} \rho_q^2 \\ &+ C \beta \rho^{\beta-1} \rho_p^2 + 2C \rho^\beta \rho_p \delta_{q,p} + \eta C_s \rho^{\eta-1}, \end{aligned} \quad (44)$$

$$\begin{aligned} P(\rho_q, T) &= \sum_q \frac{2}{3} \mathcal{E}_{Kq}(\rho_q, T) \\ &+ \frac{t_0}{2} \left(1 + \frac{x_0}{2}\right) \rho^2 + \frac{t_3}{12} \left(1 + \frac{x_3}{2}\right) (\alpha + 1) \rho^{\alpha+2} \\ &- \frac{t_0}{2} \left(\frac{1}{2} + x_0\right) \sum_q \rho_q^2 - \frac{t_3}{12} \left(\frac{1}{2} + x_3\right) (\alpha + 1) \rho^\alpha \sum_q \rho_q^2 \\ &+ C(\beta + 1) \rho^\beta \rho_p^2 + C_s(\eta - 1) \rho^\eta, \end{aligned} \quad (45)$$

$$\begin{aligned} \mathcal{E}(\rho_q, T) &= \sum_q \mathcal{E}_{Kq}(\rho_q, T) \\ &+ \frac{t_0}{2} \left(1 + \frac{x_0}{2}\right) \rho^2 - \frac{t_0}{2} \left(\frac{1}{2} + x_0\right) \sum_q \rho_q^2 + \frac{t_3}{12} \left(1 + \frac{x_3}{2}\right) \rho^{\alpha+2} - \frac{t_3}{12} \left(\frac{1}{2} + x_3\right) \rho^\alpha \sum_q \rho_q^2 \\ &+ C \rho^\beta \rho_p^2 + C_s \rho^\eta, \end{aligned} \quad (46)$$

$$T\mathcal{S}(\rho_q, T) = \sum_q \frac{5}{3} \mathcal{E}_{Kq}(\rho_q, T) - \sum_q (\mu_q - u_q) \rho_q, \quad (47)$$

$$c_P(\rho_q, T) = \frac{dQ/A}{dT} = T \left(\frac{\partial \mathcal{S}/\rho}{\partial T} \right)_P \quad \text{or} \quad c_V(\rho_q, T) = T \left(\frac{\partial \mathcal{S}/\rho}{\partial T} \right)_V \quad (48)$$

Once we evaluate $F_{1/2}(\eta)$ and $F_{3/2}(\eta)$, or more directly $\eta = F_{1/2}^{-1}(\chi)$ and $F_{3/2}(\eta)$, we can evaluate various thermodynamic quantities in terms of ρ_q and T .

For low temperature and high density limit, $\lambda^3 \rho$ large, i.e., when the average de Broglie thermal wavelength λ is larger than the average interparticle separation $\rho^{-1/3}$, we can use nearly degenerate (Fermi gas) approximations [14] for $F_{1/2}$ to obtain

$$\begin{aligned} \eta_q(\rho_q, T) &= \beta(\mu_q - u_q) = \beta \frac{p_{Fq}^2}{2m} = F_{1/2}^{-1} \left(\frac{\sqrt{\pi}}{2\gamma} \lambda^3 \rho_q \right) = \epsilon_{Fq} \left[1 - \frac{\pi^2}{12} \left(\frac{T}{\epsilon_{Fq}} \right)^2 + \dots \right] \\ &= \frac{\hbar^2}{2m} \left(\frac{6\pi^2}{\gamma} \right)^{2/3} \left[\rho_q^{2/3} - \frac{\pi^2 m^2}{3\hbar^4} \left(\frac{\gamma}{6\pi^2} \right)^{4/3} T^2 \rho_q^{-2/3} + \dots \right], \end{aligned} \quad (49)$$

$$\begin{aligned} \mathcal{E}_{Kq}(\rho_q, T) &= \frac{2\gamma}{\beta\sqrt{\pi}} \lambda^{-3} F_{3/2}(\eta_q) = \frac{3}{5} \rho_q \epsilon_{Fq} \left[1 + \frac{5\pi^2}{12} \left(\frac{T}{\epsilon_{Fq}} \right)^2 + \dots \right] \\ &= \frac{3\hbar^2}{10m} \left(\frac{6\pi^2}{\gamma} \right)^{2/3} \left[\rho_q^{5/3} + \frac{5\pi^2 m^2}{3\hbar^4} \left(\frac{\gamma}{6\pi^2} \right)^{4/3} T^2 \rho_q^{1/3} + \dots \right] \end{aligned} \quad (50)$$

In the other limit where $\lambda^3 \rho$ is small, we have a nearly non-degenerate Fermi gas (classical ideal gas) and the resulting equations are given by an ideal gas in leading order with higher order corrections [14] as

$$\eta_q(\rho_q, T) = \beta(\mu_q - u_q) = \ln \left[\frac{\rho_q \lambda^3}{\gamma} \left(1 + \frac{1}{2\sqrt{2}} \frac{\rho_q \lambda^3}{\gamma} + \dots \right) \right] \approx \ln \left(\frac{\rho_q \lambda^3}{\gamma} \right) + \frac{1}{2\sqrt{2}} \left(\frac{\rho_q \lambda^3}{\gamma} \right), \quad (51)$$

$$\mathcal{E}_{Kq}(\rho_q, T) = \frac{2}{3} P_{Kq} = \frac{2}{3} \rho_q T \left[1 + \frac{1}{2^{5/2}} \frac{\rho_q \lambda^3}{\gamma} + \left(\frac{1}{8} - \frac{2}{3^{5/2}} \right) \left(\frac{\rho_q \lambda^3}{\gamma} \right)^2 + \dots \right] \quad (52)$$

For a nuclear system with protons and neutrons with the interaction given by Eq.(34), the non-degenerate Fermi gas limit of Eqs.(51) and (52) leads to the following set of equations

$$\begin{aligned}
\mu_q(\rho, y, T) &= T \ln \left[\left(\frac{\lambda^3}{\gamma} \right) \rho_q \right] + \frac{T}{2\sqrt{2}} \left(\frac{\lambda^3}{\gamma} \right) \rho_q \\
&\quad + t_0 \left(1 + \frac{x_0}{2} \right) \rho + \frac{t_3}{12} \left(1 + \frac{x_3}{2} \right) (\alpha + 2) \rho^{\alpha+1} - \frac{t_3}{12} \left(\frac{1}{2} + x_3 \right) \alpha \rho^{\alpha+1} \\
&\quad - t_0 \left(\frac{1}{2} + x_0 \right) \rho_q + \frac{t_3}{12} \left(\frac{1}{2} + x_3 \right) (\alpha - 1) 2 \rho^\alpha \rho_q - \frac{t_3}{12} \left(\frac{1}{2} + x_3 \right) 2 \alpha \rho^{\alpha-1} \rho_q^2 \\
&\quad + C \beta \rho^{\beta-1} \rho_p^2 + 2C \rho^\beta \rho_p \delta_{q,p} + \eta C_s \rho^{\eta-1} \\
&= T \ln \left[\left(\frac{\lambda^3}{\gamma} \right) \left(\frac{\rho}{2} \pm (2y-1) \left(\frac{\rho}{2} \right) \right) \right] \\
&\quad + \frac{T}{2\sqrt{2}} \left(\frac{\lambda^3}{\gamma} \right) \left[\frac{\rho}{2} \pm (2y-1) \frac{\rho}{2} \right] + \frac{3}{4} t_0 \rho \mp \left(\frac{1}{2} + x_0 \right) t_0 (2y-1) \left(\frac{\rho}{2} \right) \\
&\quad + \frac{(\alpha+2)}{16} t_3 \rho^{\alpha+1} - \frac{1}{6} \left(\frac{1}{2} + x_3 \right) t_3 \left[\alpha (2y-1)^2 \left(\frac{\rho}{2} \right)^2 \pm (2y-1) \left(\frac{\rho}{2} \right) \rho \right] \rho^{\alpha-1} \\
&\quad + \frac{1}{4} C [\beta + 2(1 \pm 1)] \rho^{\beta+1} + C \left[(\beta + 1 \pm 1) (2y-1) \left(\frac{\rho}{2} \right) \rho + \beta (2y-1)^2 \left(\frac{\rho}{2} \right)^2 \right] \rho^{\beta-1} \\
&\quad + \eta C_s \rho^{\eta-1}, \tag{53}
\end{aligned}$$

$$\begin{aligned}
P(\rho, y, T) &= T \rho + \frac{T}{2\sqrt{2}} \left(\frac{\lambda^3}{\gamma} \right) \left(\frac{\sum_q \rho_q^2}{2} \right) \\
&\quad + \frac{t_0}{2} \left(1 + \frac{x_0}{2} \right) \rho^2 + \frac{t_3}{12} \left(1 + \frac{x_3}{2} \right) (\alpha + 1) \rho^{\alpha+2} \\
&\quad - \frac{t_0}{2} \left(\frac{1}{2} + x_0 \right) \sum_q \rho_q^2 - \frac{t_3}{12} \left(\frac{1}{2} + x_3 \right) (\alpha + 1) \rho^\alpha \sum_q \rho_q^2 \\
&\quad + C(\beta + 1) \rho^\beta \rho_p^2 + C_s(\eta - 1) \rho^\eta \\
&= T \rho + \frac{3}{8} t_0 \rho^2 + \frac{(\alpha+1)}{16} t_3 \rho^{\alpha+2} + \frac{T}{2\sqrt{2}} \left(\frac{\lambda^3}{\gamma} \right) \left(\frac{\rho}{2} \right)^2 + \frac{(\beta+1)}{4} C \rho^{\beta+2} + (\eta - 1) C_s \rho^\eta \\
&\quad - \left[t_0 \left(\frac{1}{2} + x_0 \right) + \left(\frac{\alpha+1}{6} \right) t_3 \left(\frac{1}{2} + x_3 \right) \rho^\alpha - \frac{kT}{2\sqrt{2}} \left(\frac{\lambda^3}{\gamma} \right) - (\beta + 1) C \rho^\beta \right] (2y-1)^2 \left(\frac{\rho}{2} \right)^2 \\
&\quad + (\beta + 1) C \rho^{\beta+1} (2y-1) \left(\frac{\rho}{2} \right), \tag{54}
\end{aligned}$$

$$\begin{aligned}
\mathcal{E}(\rho, y, T) &= \frac{3}{2} T \rho + \frac{3}{2} \frac{T}{2\sqrt{2}} \left(\frac{\lambda^3}{\gamma} \right) \left(\frac{\sum_q \rho_q^2}{2} \right) \\
&\quad + \frac{t_0}{2} \left(1 + \frac{x_0}{2} \right) \rho^2 - \frac{t_0}{2} \left(\frac{1}{2} + x_0 \right) \sum_q \rho_q^2 + \frac{t_3}{12} \left(1 + \frac{x_3}{2} \right) \rho^{\alpha+2} - \frac{t_3}{12} \left(\frac{1}{2} + x_3 \right) \rho^\alpha \sum_q \rho_q^2 \\
&\quad + C \rho^\beta \rho_p^2 + C_s \rho^\eta \\
&= \frac{3}{2} T \rho + \frac{3}{8} t_0 \rho^2 + \frac{1}{16} t_3 \rho^{\alpha+2} + \frac{3}{2} \frac{T}{2\sqrt{2}} \left(\frac{\lambda^3}{\gamma} \right) \left(\frac{\rho}{2} \right)^2 + \frac{1}{4} C \rho^{\beta+2} + C_s \rho^\eta \\
&\quad - \left[t_0 \left(\frac{1}{2} + x_0 \right) + \left(\frac{1}{6} \right) t_3 \left(\frac{1}{2} + x_3 \right) \rho^\alpha - \frac{3}{2} \frac{kT}{2\sqrt{2}} \left(\frac{\lambda^3}{\gamma} \right) - C \rho^\beta \right] (2y-1)^2 \left(\frac{\rho}{2} \right)^2 \\
&\quad + C \rho^{\beta+1} (2y-1) \left(\frac{\rho}{2} \right), \tag{55}
\end{aligned}$$

$$\begin{aligned}
TS(\rho, y, T) &= \frac{5}{2} T \rho - T \sum_q \rho_q \ln \left(\frac{\lambda^3}{\gamma} \rho_q \right) + \frac{T}{2\sqrt{2}} \left(\frac{\lambda^3}{\gamma} \right) \left(\frac{\sum_q \rho_q^2}{4} \right) \\
&= T \rho \left[\frac{5}{2} - y \ln \left(\frac{\lambda^3}{\gamma} y \rho \right) - (1-y) \ln \left(\frac{\lambda^3}{\gamma} (1-y) \rho \right) \right]
\end{aligned}$$

$$+\frac{T}{2\sqrt{2}}\left(\frac{\lambda^3}{\gamma}\right)\frac{[1+(2y-1)^2]}{2}\left(\frac{\rho}{2}\right)^2 \quad (56)$$

Here, for the proton density (ρ_p) and neutron density (ρ_n), we defined,

$$\begin{aligned} \rho &= \rho_p + \rho_n, & \rho_3 &= \rho_p - \rho_n = (2y-1)\rho, & y &= \rho_p/\rho, \\ \rho_p &= \frac{1}{2}(\rho + \rho_3) = y\rho, & \rho_n &= \frac{1}{2}(\rho - \rho_3) = (1-y)\rho, \\ \sum_q \rho_q^2 &= \frac{1}{2}(\rho^2 + \rho_3^2) = \frac{[1+(2y-1)^2]}{2}\rho^2 = [1+2y(y-1)]\rho^2, \\ \sum_q \rho_q^3 &= \frac{1}{4}\rho(\rho^2 + 3\rho_3^2) = \frac{[1+3(2y-1)^2]}{4}\rho^3 = [1+3y(y-1)]\rho^3 \end{aligned} \quad (57)$$

The \pm in μ_q stands $+$ for q =proton and $-$ for neutron. For $x_3 \neq -1/2$ and $C \neq 0$, the $P(\rho)$ curve for different vales of y at fixed T may cross at some density ρ which was not seen in Ref. [7].

For a constant T and constant P , ρ and y are not independent. Pressure P of Eq.(54) is a second order polynomial of $(2y-1)\left(\frac{\rho}{2}\right)$, and thus we have, for the range of $0 \leq y \leq 1/2$,

$$\begin{aligned} -1 \leq (2y-1) &= \frac{(\beta+1)C\rho^\beta}{\left(\frac{1}{2}+x_0\right)t_0 + \left(\frac{\alpha+1}{6}\right)\left(\frac{1}{2}+x_3\right)t_3\rho^\alpha - (\beta+1)C\rho^\beta - \frac{kT}{2\sqrt{2}}\left(\frac{\lambda^3}{\gamma}\right)} \\ &\mp \frac{2}{\rho} \left[\left(\frac{(\beta+1)C\rho^\beta}{\left(\frac{1}{2}+x_0\right)t_0 + \left(\frac{\alpha+1}{6}\right)\left(\frac{1}{2}+x_3\right)t_3\rho^\alpha - (\beta+1)C\rho^\beta - \frac{kT}{2\sqrt{2}}\left(\frac{\lambda^3}{\gamma}\right)} \right)^2 \left(\frac{\rho}{2}\right)^2 \right. \\ &\quad \left. + \frac{T\rho + \frac{3}{8}t_0\rho^2 + \frac{(\alpha+1)}{16}t_3\rho^{\alpha+2} + \frac{(\beta+1)}{4}C\rho^{\beta+2} + (\eta-1)C_s\rho^\eta + \frac{T}{2\sqrt{2}}\left(\frac{\lambda^3}{\gamma}\right)\frac{\rho^2}{4} - P}{\left(\frac{1}{2}+x_0\right)t_0 + \left(\frac{\alpha+1}{6}\right)\left(\frac{1}{2}+x_3\right)t_3\rho^\alpha - (\beta+1)C\rho^\beta - \frac{T}{2\sqrt{2}}\left(\frac{\lambda^3}{\gamma}\right)} \right]^{1/2} \leq 0 \end{aligned} \quad (58)$$

for a given density ρ . (Here $+$ sign is allowed for the case that the first term is negative.) Without the Coulomb interaction only the second term in the square root survives and $y(\rho)$ is a single valued function of ρ in the range of $0 \leq y \leq 1/2$. The numerator of the second term in the square root is $P(\rho, y=1/2, T) - P(\rho, y, T)$, i.e., the negative of the pressure measured with respect to the pressure for a symmetric nuclear system. Notice here that t_0 is negative and $P(y) \geq P(y=1/2)$ for the potential without the Coulomb interaction (see Eq.(54)). Since we are considering only $-1 \leq (2y-1) \leq 0$, we have conditions of

$$\begin{aligned} 0 &\leq \frac{T\rho + \frac{3}{8}t_0\rho^2 + \frac{(\alpha+1)}{16}t_3\rho^{\alpha+2} + \frac{(\beta+1)}{4}C\rho^{\beta+2} + (\eta-1)C_s\rho^\eta + \frac{T}{2\sqrt{2}}\left(\frac{\lambda^3}{\gamma}\right)\frac{\rho^2}{4} - P}{\left(\frac{1}{2}+x_0\right)t_0 + \left(\frac{\alpha+1}{6}\right)\left(\frac{1}{2}+x_3\right)t_3\rho^\alpha - (\beta+1)C\rho^\beta - \frac{T}{2\sqrt{2}}\left(\frac{\lambda^3}{\gamma}\right)} \\ &\leq \left[\frac{2(\beta+1)C\rho^\beta}{\left(\frac{1}{2}+x_0\right)t_0 + \left(\frac{\alpha+1}{6}\right)\left(\frac{1}{2}+x_3\right)t_3\rho^\alpha - (\beta+1)C\rho^\beta - \frac{T}{2\sqrt{2}}\left(\frac{\lambda^3}{\gamma}\right)} + 1 \right] \left(\frac{\rho}{2}\right)^2 \end{aligned} \quad (59)$$

to have $0 \leq y \leq 1/2$ of which the boundaries are related to the pressures at $y=1/2$ and $y=0$ respectively. For non-zero C , there is a back bending in $y(\rho)$. This behavior is related to the choice of opposite sign for the square root term in Eq.(58) and double values of y for a given ρ . To find the point of back bending, we look at the $(\partial\rho/\partial y)_{T,P} = 0$ point. Using Eq.(58) we can find the energy and entropy as a function of pressure P , proton fraction y , and temperature T , i.e., $\mathcal{E}(P, y, T)$ and $\mathcal{S}(P, y, T)$. From these results we may study an isobaric phase transition. Since all the phases have the same pressure in the coexistent region, $\mu_q(P, y, T)$ may be used to find the coexistent region.

At fixed T and P , only one of either ρ or y is the independent variable. Thus observables such as P , \mathcal{E}/ρ , \mathcal{S}/ρ may have a discontinuity in T or y when $\left(\frac{\partial\rho}{\partial T}\right)_{y,P}$ or $\left(\frac{\partial\rho}{\partial y}\right)_{T,P}$ diverges. We can study the behavior of thermodynamic quantities at a fixed P using $dP=0$ from Eq.(54),

$$\begin{aligned} dP &= \left\{ \left[T\rho - \frac{T}{2\sqrt{2}}\left(\frac{\lambda^3}{\gamma}\right)\left(\frac{\sum_q \rho_q^2}{4}\right) \right] \right\} \frac{dT}{T} \\ &+ \left\{ \left[T\rho + \frac{T}{2\sqrt{2}}\left(\frac{\lambda^3}{\gamma}\right)\left(\sum_q \rho_q^2\right) \right] \right\} \end{aligned}$$

$$\begin{aligned}
& + \left[t_0 \left(1 + \frac{x_0}{2} \right) \rho^2 + \frac{t_3}{12} \left(1 + \frac{x_3}{2} \right) (\alpha + 1)(\alpha + 2) \rho^{\alpha+2} \right. \\
& - t_0 \left(\frac{1}{2} + x_0 \right) \left(\sum_q \rho_q^2 \right) - \frac{t_3}{12} \left(\frac{1}{2} + x_3 \right) (\alpha + 1)(\alpha + 2) \rho^\alpha \left(\sum_q \rho_q^2 \right) \\
& \left. + C(\beta + 1)(\beta + 2) \rho^\beta \rho_p^2 + C_s(\eta - 1) \eta \rho^\eta \right] \frac{d\rho}{\rho} \\
& - \left\{ \left[t_0 \left(\frac{1}{2} + x_0 \right) + \left(\frac{\alpha + 1}{6} \right) t_3 \left(\frac{1}{2} + x_3 \right) \rho^\alpha - (\beta + 1) C \rho^\beta - \frac{T}{2\sqrt{2}} \left(\frac{\lambda^3}{\gamma} \right) \right] \left(\frac{\rho \rho_3}{4} \right) \right. \\
& \left. + (\beta + 1) C \rho^\beta \left(\frac{\rho}{2} \right)^2 \right\} 4dy \\
& = \left\{ \left[\rho - \frac{1}{2} \frac{1}{2\sqrt{2}} \left(\frac{\lambda^3}{\gamma} \right) \left(\frac{\rho}{2} \right)^2 - \frac{1}{2} \frac{1}{2\sqrt{2}} \left(\frac{\lambda^3}{\gamma} \right) (2y - 1)^2 \left(\frac{\rho}{2} \right)^2 \right] dT \right. \\
& + \left\{ \left[T + 2\tilde{b}_2 \rho + (\alpha + 2) \tilde{b}_3 \rho^{\alpha+1} + \frac{T}{2\sqrt{2}} \left(\frac{\lambda^3}{\gamma} \right) \left(\frac{\rho}{2} \right) + (\beta + 2) \tilde{b}_C \rho^{\beta+1} + \eta(\eta - 1) C_s \rho^{\eta-1} \right] \right. \\
& - \left[t_0 \left(\frac{1}{2} + x_0 \right) + \left(\frac{\alpha + 2}{2} \right) \left(\frac{\alpha + 1}{6} \right) t_3 \left(\frac{1}{2} + x_3 \right) \rho^\alpha - \left(\frac{\beta + 2}{2} \right) (\beta + 1) C \rho^\beta - \frac{T}{2\sqrt{2}} \left(\frac{\lambda^3}{\gamma} \right) \right] \\
& \times (2y - 1)^2 \left(\frac{\rho}{2} \right)^2 + (\beta + 2)(\beta + 1) C \rho^\beta (2y - 1) \left(\frac{\rho}{2} \right) \left. \right\} d\rho \\
& - \left\{ \left[t_0 \left(\frac{1}{2} + x_0 \right) + \left(\frac{\alpha + 1}{6} \right) t_3 \left(\frac{1}{2} + x_3 \right) \rho^\alpha - (\beta + 1) C \rho^\beta - \frac{T}{2\sqrt{2}} \left(\frac{\lambda^3}{\gamma} \right) \right] (2y - 1) \left(\frac{\rho}{2} \right)^2 \right. \\
& \left. + (\beta + 1) C \rho^\beta \left(\frac{\rho}{2} \right)^2 \right\} 4dy
\end{aligned} \tag{60}$$

Thus we have, for a fixed P and y ,

$$\begin{aligned}
\left(\frac{\partial \rho}{\partial T} \right)_{y,P} & = - \left\{ \left[T \rho - \frac{T}{2\sqrt{2}} \left(\frac{\lambda^3}{\gamma} \right) \left(\frac{\sum_q \rho_q^2}{4} \right) \right] \right\} \frac{\rho}{T} \\
& \times \left\{ \left[T \rho + \frac{T}{2\sqrt{2}} \left(\frac{\lambda^3}{\gamma} \right) \left(\sum_q \rho_q^2 \right) \right] \right. \\
& + \left[t_0 \left(1 + \frac{x_0}{2} \right) \rho^2 + \frac{t_3}{12} \left(1 + \frac{x_3}{2} \right) (\alpha + 1)(\alpha + 2) \rho^{\alpha+2} \right. \\
& - t_0 \left(\frac{1}{2} + x_0 \right) \left(\sum_q \rho_q^2 \right) - \frac{t_3}{12} \left(\frac{1}{2} + x_3 \right) (\alpha + 1)(\alpha + 2) \rho^\alpha \left(\sum_q \rho_q^2 \right) \\
& \left. \left. + C(\beta + 1)(\beta + 2) \rho^\beta \rho_p^2 + C_s(\eta - 1) \eta \rho^\eta \right] \right\}^{-1} \\
& = - \left\{ \rho - \frac{1}{2} \frac{1}{2\sqrt{2}} \left(\frac{\lambda^3}{\gamma} \right) \left(\frac{\rho}{2} \right)^2 - \frac{1}{2} \frac{1}{2\sqrt{2}} \left(\frac{\lambda^3}{\gamma} \right) (2y - 1)^2 \left(\frac{\rho}{2} \right)^2 \right\} \\
& \times \left\{ \left[T + 2\tilde{b}_2 \rho + (\alpha + 2) \tilde{b}_3 \rho^{\alpha+1} + \frac{T}{2\sqrt{2}} \left(\frac{\lambda^3}{\gamma} \right) \left(\frac{\rho}{2} \right) + (\beta + 2) \tilde{b}_C \rho^{\beta+1} + \eta(\eta - 1) C_s \rho^{\eta-1} \right] \right. \\
& - \left[t_0 \left(\frac{1}{2} + x_0 \right) + \left(\frac{\alpha + 2}{2} \right) \left(\frac{\alpha + 1}{6} \right) t_3 \left(\frac{1}{2} + x_3 \right) \rho^\alpha - \left(\frac{\beta + 2}{2} \right) (\beta + 1) C \rho^\beta - \frac{T}{2\sqrt{2}} \left(\frac{\lambda^3}{\gamma} \right) \right] \\
& \times (2y - 1)^2 \left(\frac{\rho}{2} \right)^2 + (\beta + 2)(\beta + 1) C \rho^\beta (2y - 1) \left(\frac{\rho}{2} \right) \left. \right\}^{-1}
\end{aligned} \tag{61}$$

Using this we get the specific heat capacity, from Eq.(56),

$$\begin{aligned}
c_P & = T \left(\frac{\partial S/\rho}{\partial T} \right)_{y,P} \\
& = T \left[\frac{5}{2} + \frac{3}{2} - y \ln \left(\frac{\lambda^3}{\gamma} y \rho \right) - (1 - y) \ln \left(\frac{\lambda^3}{\gamma} (1 - y) \rho \right) \right] - \frac{1}{2} \frac{T}{2\sqrt{2}} \left(\frac{\lambda^3}{\gamma} \right) \frac{[1 + (2y - 1)^2]}{2} \left(\frac{\rho}{4} \right)
\end{aligned}$$

$$\begin{aligned}
& + \left\{ -T + \frac{T}{2\sqrt{2}} \left(\frac{\lambda^3}{\gamma} \right) \frac{[1 + (2y-1)^2]}{2} \left(\frac{\rho}{4} \right) \right\} \left(\frac{1}{\rho} \right) T \left(\frac{\partial \rho}{\partial T} \right)_{y,P} \\
& = T \left[4 - y \ln \left(\frac{\lambda^3}{\gamma} y \rho \right) - (1-y) \ln \left(\frac{\lambda^3}{\gamma} (1-y) \rho \right) \right] - \frac{1}{2} \frac{T}{2\sqrt{2}} \left(\frac{\lambda^3}{\gamma} \right) \frac{[1 + (2y-1)^2]}{2} \left(\frac{\rho}{4} \right) \\
& + \left\{ T - \frac{T}{2\sqrt{2}} \left(\frac{\lambda^3}{\gamma} \right) \frac{[1 + (2y-1)^2]}{2} \left(\frac{\rho}{4} \right) \right\}^2 \\
& \times \left\{ \left[T + 2\tilde{b}_2 \rho + (\alpha+2)\tilde{b}_3 \rho^{\alpha+1} + \frac{T}{2\sqrt{2}} \left(\frac{\lambda^3}{\gamma} \right) \left(\frac{\rho}{2} \right) + (\beta+2)\tilde{b}_C \rho^{\beta+1} + \eta(\eta-1)C_s \rho^{\eta-1} \right] \right. \\
& - \left[t_0 \left(\frac{1}{2} + x_0 \right) + \left(\frac{\alpha+2}{2} \right) \left(\frac{\alpha+1}{6} \right) t_3 \left(\frac{1}{2} + x_3 \right) \rho^\alpha - \left(\frac{\beta+2}{2} \right) (\beta+1)C \rho^\beta - \frac{T}{2\sqrt{2}} \left(\frac{\lambda^3}{\gamma} \right) \right] \\
& \times (2y-1)^2 \left(\frac{\rho}{2} \right) + (\beta+2)(\beta+1)C \rho^\beta (2y-1) \left(\frac{\rho}{2} \right) \left. \right\}^{-1} \\
& = \left[4T\rho - T \sum_q \rho_q \ln \left(\frac{\lambda^3}{\gamma} \rho_q \right) - \frac{1}{2} \frac{T}{2\sqrt{2}} \left(\frac{\lambda^3}{\gamma} \right) \left(\frac{\sum_q \rho_q^2}{4} \right) \right] \left(\frac{1}{\rho} \right) \\
& + \left\{ \left[T\rho - \frac{T}{2\sqrt{2}} \left(\frac{\lambda^3}{\gamma} \right) \left(\frac{\sum_q \rho_q^2}{4} \right) \right] \right\}^2 \left(\frac{1}{\rho} \right) \\
& \times \left\{ \left[kT\rho + \frac{T}{2\sqrt{2}} \left(\frac{\lambda^3}{\gamma} \right) \left(\sum_q \rho_q^2 \right) \right] + \left[t_0(1 + \frac{x_0}{2})\rho^2 - t_0(\frac{1}{2} + x_0) \left(\sum_q \rho_q^2 \right) \right. \right. \\
& + \frac{t_3}{12}(1 + \frac{x_3}{2})(\alpha+1)(\alpha+2)\rho^{\alpha+2} - \frac{t_3}{12}(\frac{1}{2} + x_3)(\alpha+1)(\alpha+2)\rho^\alpha \left. \left(\sum_q \rho_q^2 \right) \right. \\
& \left. \left. + C(\beta+1)(\beta+2)\rho^\beta \rho_p^2 + C_s(\eta-1)\eta\rho^\eta \right] \right\}^{-1}, \tag{62} \\
c_V & = T \left(\frac{\partial \mathcal{S}/\rho}{\partial T} \right)_{y,V} \\
& = T \left[4 - y \ln \left(\frac{\lambda^3}{\gamma} y \rho \right) - (1-y) \ln \left(\frac{\lambda^3}{\gamma} (1-y) \rho \right) \right] - \frac{1}{2} \frac{T}{2\sqrt{2}} \left(\frac{\lambda^3}{\gamma} \right) \frac{[1 + (2y-1)^2]}{2} \left(\frac{\rho}{4} \right) \\
& = \left[4T\rho - T \sum_q \rho_q \ln \left(\frac{\lambda^3}{\gamma} \rho_q \right) - \frac{1}{2} \frac{T}{2\sqrt{2}} \left(\frac{\lambda^3}{\gamma} \right) \left(\frac{\sum_q \rho_q^2}{4} \right) \right] \left(\frac{1}{\rho} \right) \tag{63}
\end{aligned}$$

This shows that there is a divergence of c_P at T with $\left(\frac{\partial \rho}{\partial T} \right)_{y,P} = \infty$, i.e., $\left(\frac{\partial T}{\partial \rho} \right)_{y,P} = 0$ showing first order phase transition. This happens when $\left(\frac{\partial y}{\partial \rho} \right)_{T,P} = 0$ which may exist in the coexist region. The specific heat with fixed volume c_V has no divergence.

III. PHASE TRANSITION OF A FINITE NUCLEUS WITH COULOMB INTERACTION

Here we use Skyrme interaction of PRC45 in Table I with $\beta = 0$, $\eta = 2/3$, the surface energy $4\pi r_0^2 \sigma = 20.0$ MeV, and $R = 6$ fm. Fig.1 shows the pressure $P(\rho)$ for various y values at $T = 10$ MeV. With $x_3 = -1/2$, there is no crossing of $P(\rho)$ curves between different values of y at fixed T which is a behavior similar to that in Ref. [7]. However, for $T = 10$ MeV, the lowest pressure occurs not at $y = 1/2$ but at $y = 0.4552$ for $R = 6$ fm due to the Coulomb repulsion independent of the surface tension (see Eq.(54)). For $R = 10$ fm, the lowest pressure occurs at $y = 0.3927$.

For fixed P and T , y and ρ are not independent. Since Eq.(54) is a second order equation for y , y can have two values for a given density ρ in general. Fig.2 shows $y(\rho)$ for various P values at $T = 10$ MeV. Here only the $0 \leq y \leq 0.5$ region is shown. These curves show back bending for large y with $\frac{\partial \rho}{\partial y} = 0$ at $y = 0.4552 < 1/2$ for the parameter with Coulomb interaction which is used here. At this y value the pressure is minimum as mentioned above. Without Coulomb interaction, there is no back bending in the $0 \leq y \leq 0.5$ region and $\frac{\partial \rho}{\partial y} = 0$ at $y = 1/2$. The discontinuity of $y(\rho)$ at low density for small pressure is expected from the low density region of Fig.1.

Fig.3 shows chemical potential $\mu_q(y)$ for various P values at $T = 10$ MeV. From this figure we can find binodal points by checking the condition Eq.(32). There is a cross between the small density portion and high density portion of the curves for low pressure (see the box at the right-bottom corner of Fig.3), which has a discontinuity in $y(\rho)$ shown in Fig.2, for both μ_p and μ_n . The overall behavior is qualitatively similar to the result of Ref. [7]. However with Coulomb interaction $\mu_n < \mu_p$ at $y = 1/2$ instead of $\mu_n = \mu_p$. The existence of these crossings of chemical potential curves between high and low density and between proton and neutron allow two pairs of binodal points at low P as shown in the box at the right-upper corner of Fig.4.

Fig.4 shows the coexistence binodal curve in y - P plane at $T = 10$ MeV. The figure shows that the major effect of the surface tension is a lowering of the pressure for the coexistence curve (compare dash-dotted curve *vs* dashed curve and solid curve *vs* dash-dot-dot-dotted curve). Inclusion of surface tension may allow for a zero pressure isobaric phase transition and may simulate the situation of an equilibrated state of multifragmentation having zero internal pressure of stable finite nuclei with non-zero gas pressure as discussed in Ref. [9]. The effect of the Coulomb interaction makes the coexistence curve smaller. However the more important effect of Coulomb interaction is the appearance of another pair of binodal points in the low pressure region (see the expanded figure in the box at the right upper corner). Two points of smaller y values have the same chemical potential and two points of larger y values have the same chemical potential but which are different (having increased μ_p and decreased μ_n) from the other two (see Table II). Here the points with largest and smallest y value are in gas phase and the points between the other two y values are in the liquid phase (see Table II). The binodal pair with higher y values allows the mixture of gas with highest y and liquid with the next high y and is a reversed situation from the other binodal pairs and the result of Ref. [7]. This allows for a phase separation into a liquid phase with less proton (lower y value) and a gas phase with more proton (higher y value) which is more realistic in heavy ion collision. Two pairs of binodal points meet together with the lowest pressure of the binodal curve at one point with $y = 0.4552$ for $R = 6$ fm which would be changed to $y = 0.3927$ for $R = 10$ fm. Without Coulomb interaction, the lowest pressure of the binodal curve occurs at $y = 1/2$.

Fig.5 shows $T(\rho)$ for various P values at $y = 0.3$ and 0.5 . This figure shows that at a low pressure there are two points with $\frac{\partial T}{\partial \rho} = 0$ which make thermodynamic quantities have a first order discontinuity with T variations.

Fig.6 and Fig.7 shows $\mathcal{E}(T)/\rho$ and $\mathcal{S}(T)/\rho$ for various P values at $y = 0.3$ and 0.5 . Comparing with the exact result (dotted curve in Fig.6), the Fermi gas approximation used here is good for the region which corresponds to $\mathcal{E}/\rho > 8$ MeV for the case without Coulomb and surface effects. The points with diverging slope of \mathcal{E}/ρ and \mathcal{S}/ρ in variations with T are related to the zero slope points in Fig.5. If the charge concentration y was kept constant in all phases then these two diverging points might be outside of the coexist region and cause a first order phase transition. However in the actual phase transition of a heavy ion collision these diverging points belong to the coexistence region and gives a second order phase transition as in Ref. [7].

IV. SUMMARY AND CONCLUSION

In this paper we studied the liquid-gas phase transition in a hadronic system made of protons and neutrons or having two components. The approach used here was based on a mean field theory and we calculated the mean potential energy using a Skryme interaction. The work is an extension of a previous study initially begone in Ref. [1] for two components and the analysis is similar in some ways to that developed in Ref. [7]. However, in this paper we included surface and Coulomb effects so our results differ quantitatively from those in Ref. [7]. Including Coulomb and surface effects introduces some feature also not present in Ref. [7].

The importance of surface energies in the liquid-gas phase transition was shown in Ref. [3,4] using an approach based on a statistical model of multifragmentation. In the statistical model of multifragmentation, because nuclear matter can be broken into a large number of small pieces, the surface energy plays a very dominant role. Here, in a mean field theory, the surface energy plays a lesser role since we do not allow for the possibility of multifragmentation. Rather, the system is treated as uniform but with varying density. Surface tension here brings the coexistence binodal surface to lower pressure which could allow an isobaric transition at zero pressure.

Inclusion of Coulomb interaction brings a new feature in a mean field approach. The Coulomb interaction makes the binodal surface smaller and cause another pair of binodal points at low pressure with a reversed proton fraction in the liquid-gas phase, i.e. with less protons in liquid phase and more protons in gas phase. The value of the proton fraction y for the liquid phase of this binodal pair is larger than the y values for the lowest pressure point of the binodal curve as can be seen in the box in Fig.4 and we can make this value smaller by using a stronger Coulomb interaction.

In this paper we used a fixed value of R to determine the strength of Coulomb interaction and surface tension. If we allow for variations of R with ρ or T and allow different values for the Coulomb and surface energies, then this simple model may be used to study multifragmentation with various size of clusters.

This research was supported by the U.S. DOE, Grant No. DE-FG02-96ER-40987. S.J. Lee gratefully acknowledges travel support for a sabbatical leave from Kyung Hee University and spent a sabbatical year at Rutgers University in 1999–2000.

-
- * Permanent address: Physics Department, School of Electronics and Information, Kyung Hee University, 1 Seochunli, Yoninsi, Kyunggido, Korea.
- [1] H.R. Jaqaman, A.Z. Mekjian, and L. Zamick, Phys. Rev. **C29**, 2067 (1984).
 - [2] J.E. Finn *et al*, Phys. Rev. Lett. **49**, 1321 (1982).
 - [3] A.S. Hirsch *et al*, Phys. Rev. **C29**, 508 (1984).
 - [4] L.P. Csernai and J.I. Kapusta, Phys. Rep. **131**, 223 (1986).
 - [5] W. Lynch, Ann. Rev. Nucl. Science **37**, 493 (1987).
 - [6] S. Das Gupta, A.Z. Mekjian, and B. Tsang, to be published in *Advances in Nuclear Physics*, Eds J. Negele and E. Vogt.
 - [7] H. Müller and B.D. Serot, Phys. Rev. **C52**, 2072 (1995).
 - [8] N.K. Glendenning, Phys. Rev. **D46**, 1274 (1992).
 - [9] S.J. Lee and A.Z. Mekjian, Phys. Rev. **C56**, 2621 (1997).
 - [10] G.F. Bertsch and S. Das Gupta, Phys. Rep. **160**, 189 (1988).
 - [11] P. Ring and P. Schuck, *The Nuclear Many-Body Problem* (Springer-Verlag, New York, 1980); S.J. Lee, Phys. Rev. **C42**, 610 (1990).
 - [12] C. Gale, G.M. Welke, M. Prakash, S.J. Lee, and S. Das Gupta, Phys. Rev. **C41**, 1545 (1990).
 - [13] S.J. Lee and A.Z. Mekjian, Phys. Rev. **C45**, 1284 (1992).
 - [14] K. Huang, *Statistical Mechanics*, (John Wiley & Sons, New York, 1987).
 - [15] S. Das Gupta and A.Z. Mekjian, Phys. Rev. **C57**, 1361 (1998).
 - [16] P. Bhattacharyya, S. Das Gupta, and A.Z. Mekjian, Phys. Rev. **C60**, 064625 (1999).

TABLE I. Parameter sets for Skyrme interaction [1,13].

Force	α	t_0 (MeV·fm ³)	x_0	t_3 (MeV·fm ^{3(1+α)})	x_3
PRC45	1	$\frac{4}{3}C_1 = -1089.0$	1/2	$\frac{16}{\alpha+2}C_2 = 17480.4$	-1/2
ZR1	1	-1003.9	0.0, 0.2, 0.5	13287.2	1.0
ZR2	2/3	-1192.2	0.0, 0.2, 0.5	11041.0	1.0
ZR3	0.1	-4392.2	0.0, 0.2, 0.5	26967.3	1.0

TABLE II. Coexistence points.

P (MeV/fm ³)	ρ (fm ³)	y	μ_p (MeV)	μ_n (MeV)
0.01496	0.0034324	0.4526870	-15.73360	-13.80920
	0.1138296	0.4548638	-15.73360	-13.80920
	0.1138296	0.4555570	-15.59369	-13.92612
	0.0034324	0.4577830	-15.59369	-13.92612
0.01498	0.0034352	0.4441228	-15.97430	-13.61531
	0.1138098	0.4536912	-15.97430	-13.61531
	0.1138096	0.4567391	-15.35914	-14.12939
	0.0034352	0.4665239	-15.35914	-14.12939
0.01500	0.0034373	0.4253351	-16.50124	-13.19126
	0.1137651	0.4511254	-16.50124	-13.19126
	0.1137652	0.4592869	-14.85386	-14.56769
	0.0034372	0.4853333	-14.85386	-14.56769
0.01503	0.0034421	0.4226954	-16.57709	-13.12985
	0.1137598	0.4507550	-16.57709	-13.12985
	0.1137592	0.4596993	-14.77187	-14.63844
	0.0034420	0.4883935	-14.77187	-14.63844
0.01505	0.0034449	0.4141177	-16.81862	-12.93537
	0.1137397	0.4495787	-16.81862	-12.93537
	0.1137389	0.4608853	-14.53660	-14.84241
	0.0034448	0.4971483	-14.53660	-14.84241
0.01506	0.0034463	0.4102457	-16.92777	-12.84748
	0.1137306	0.4490471	-16.92777	-12.84748

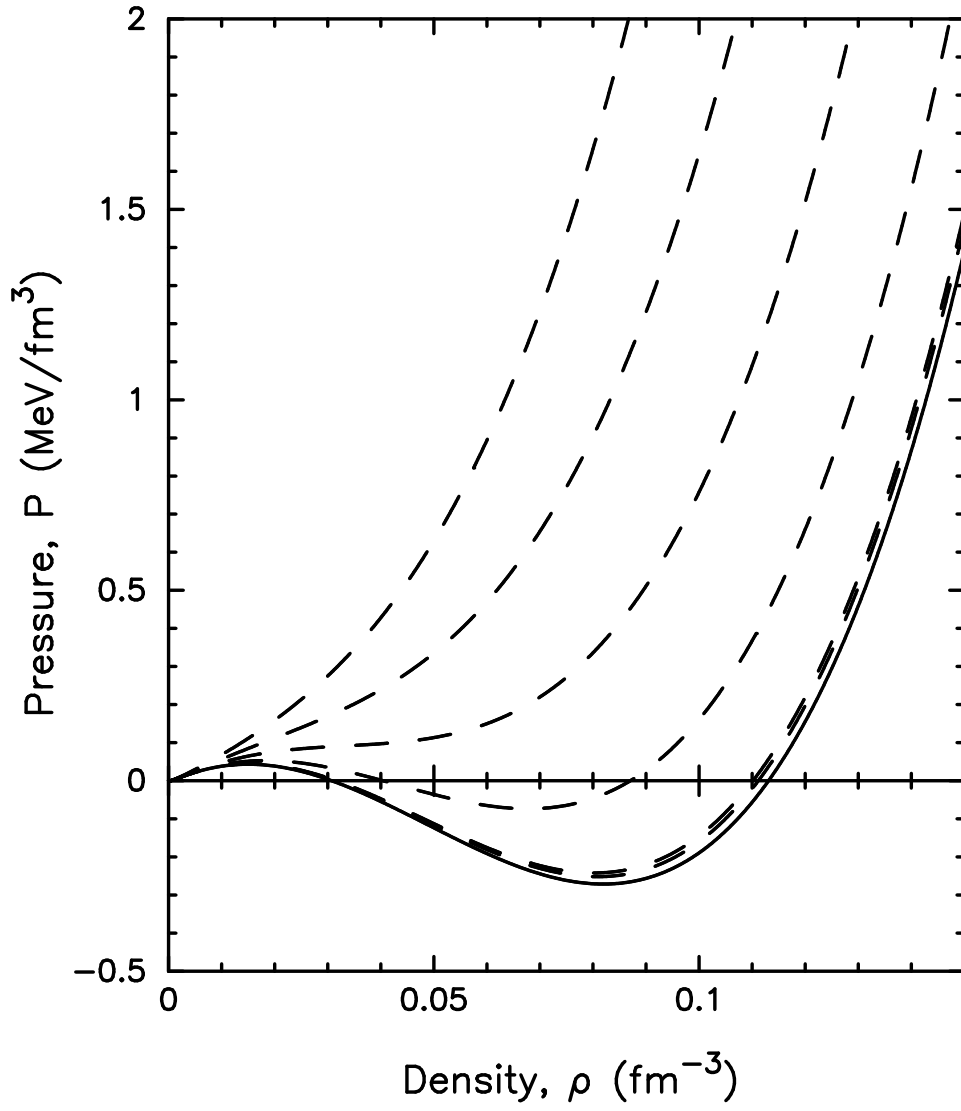


FIG. 1. Pressure $P(\rho)$ versus ρ at $T = 10$ MeV for various y . The dashed curves from top to bottom have $y = 0, 0.1, 0.2, 0.3, 0.4$, and 0.5 while the solid curve is for $y = 0.4552$.

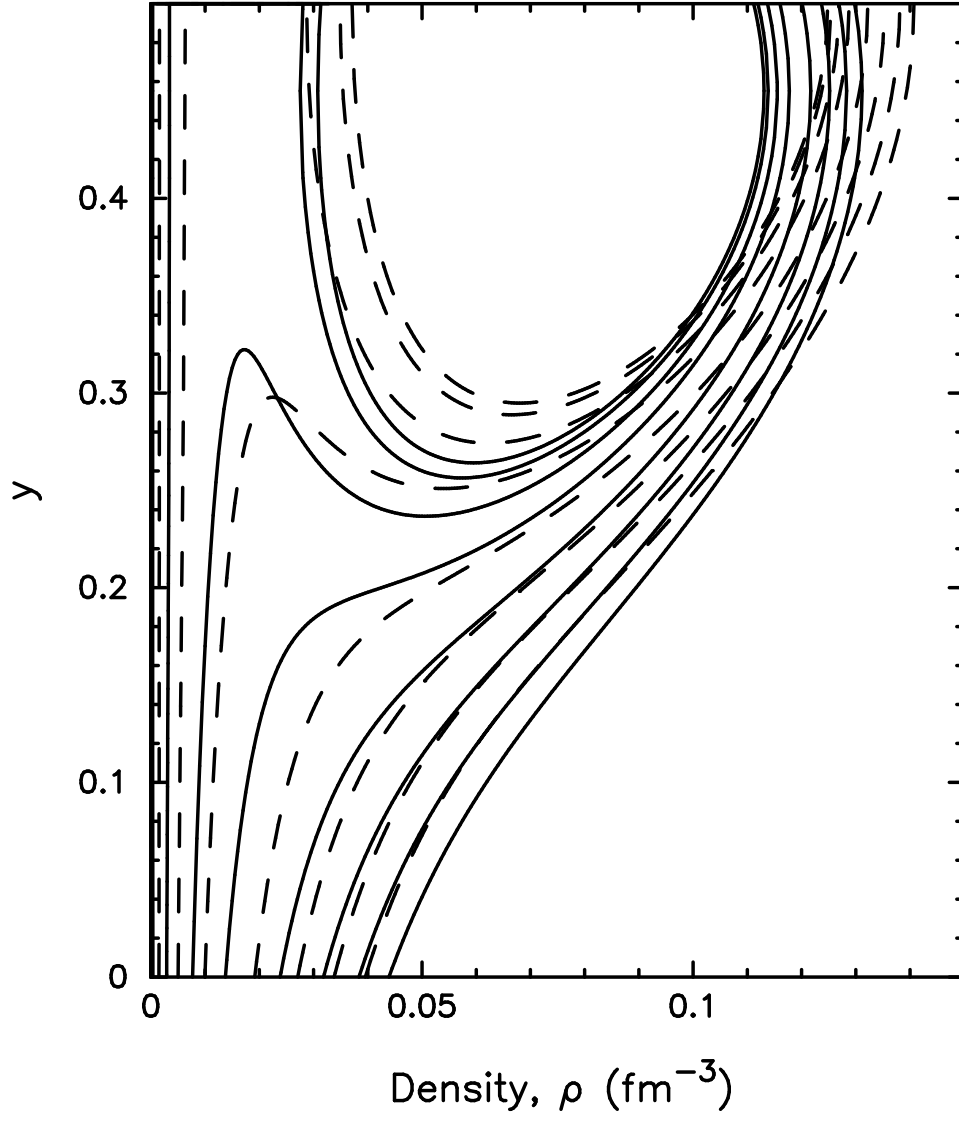


FIG. 2. Proton fraction $y(\rho)$ for $P = 0, 0.015, 0.05, 0.1, 0.2, 0.3, 0.4$, and 0.5 , from top to bottom, at $T = 10$ MeV. The solid curves have Coulomb and surface tension contributions and the dashed curves are without these interactions.

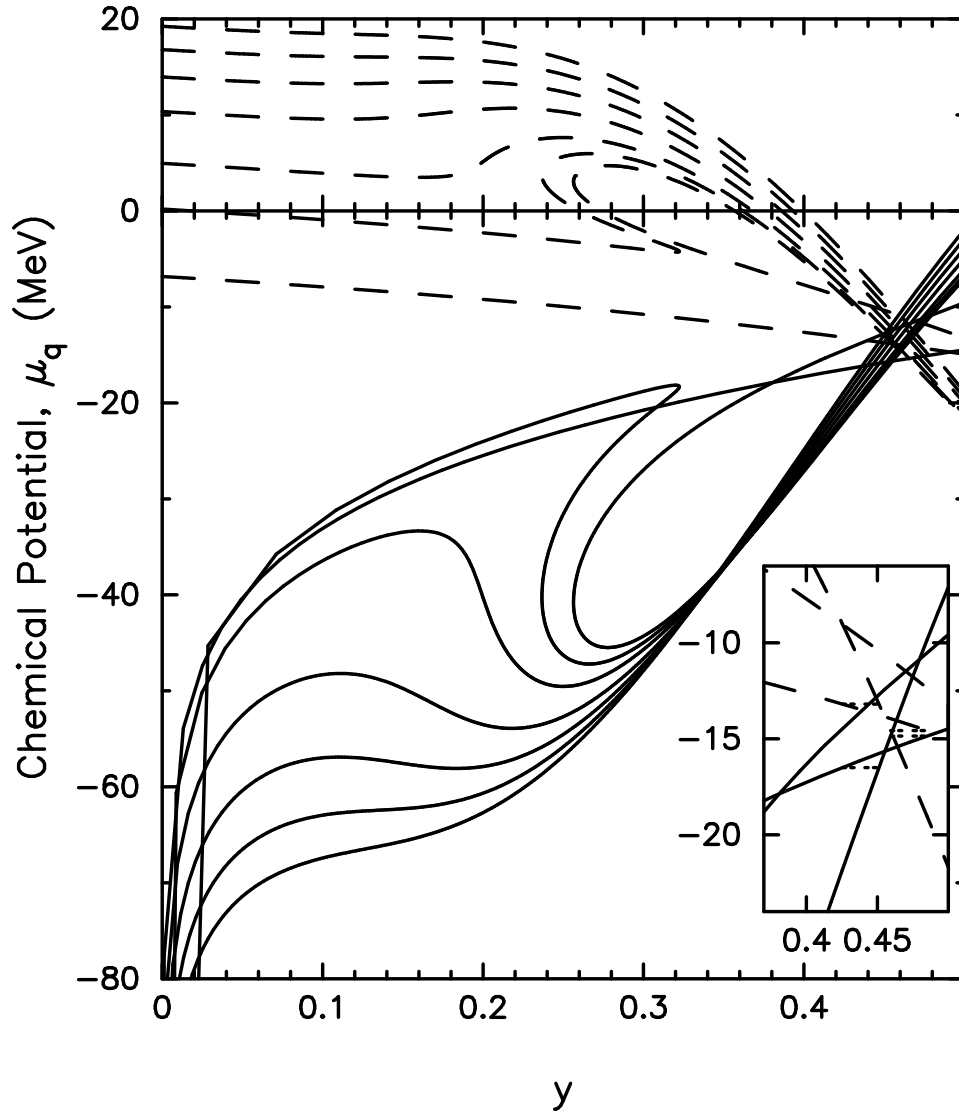


FIG. 3. Chemical potential $\mu_p(y)$ and $\mu_n(y)$ for $P = 0.015, 0.05, 0.1, 0.2, 0.3, 0.4$, and 0.5 , from top to bottom curve for proton (solid curve) and bottom to top for neutron (dashed curve) at $T = 10$ MeV. Chemical potential increases as pressure increase at $y = 1/2$. μ_n increases and μ_p decreases as P increases except μ_p for $P > 0.05$ or 0.1 for smaller y . The small box at the right-bottom corner is the expanded curve for $P = 0.015$ MeV with two pairs of binodal points indicated by dotted lines.

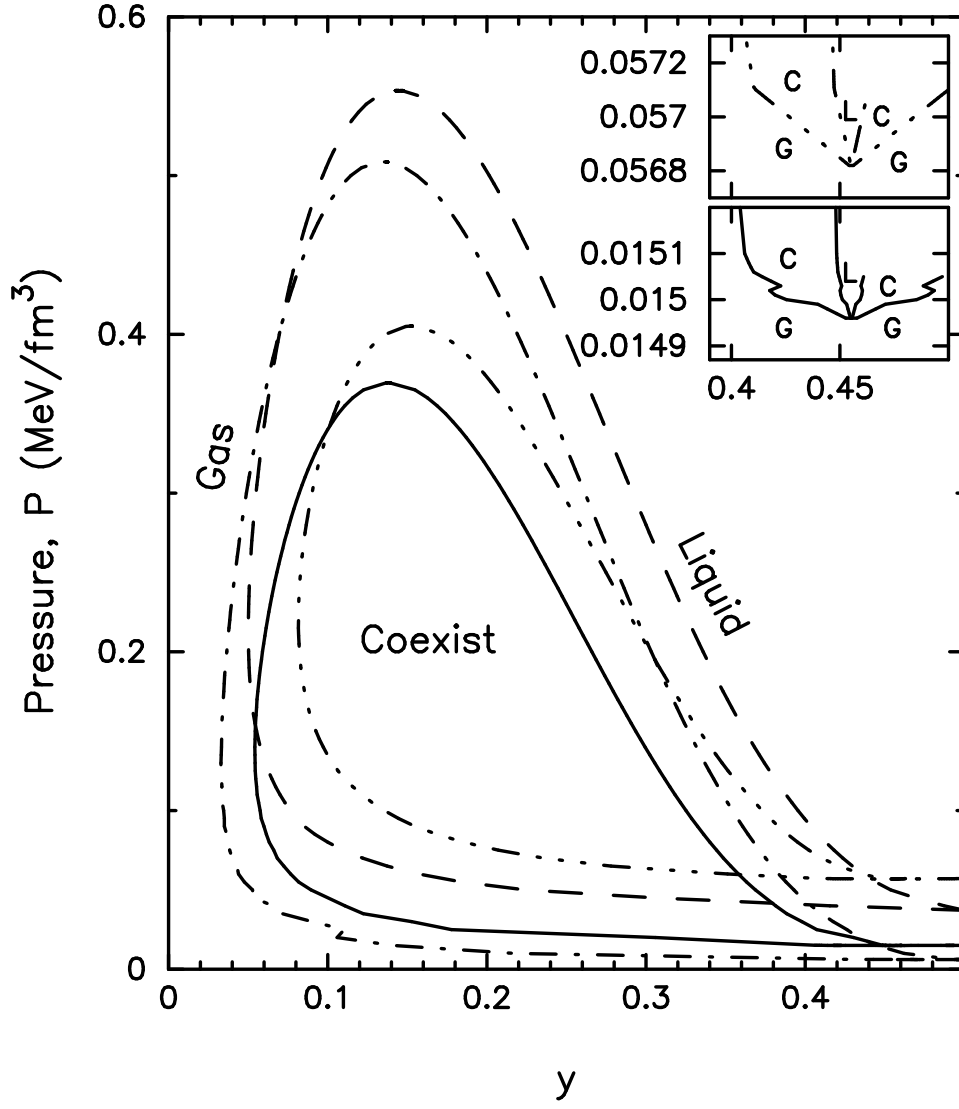


FIG. 4. Binodal curve at $T = 10$ MeV. The solid curve is for the case with Coulomb and surface effect, the dash-dotted curve is for the case with Coulomb interaction, the dash-dot-dot-dotted curve is for the case with surface effect, and the dashed curve is for the case without Coulomb and surface effect. Small boxes at the upper right corner are the expansion of the main figure. In small boxes, the region of liquid, gas, and coexistence are indicated by L, G, and C respectively.

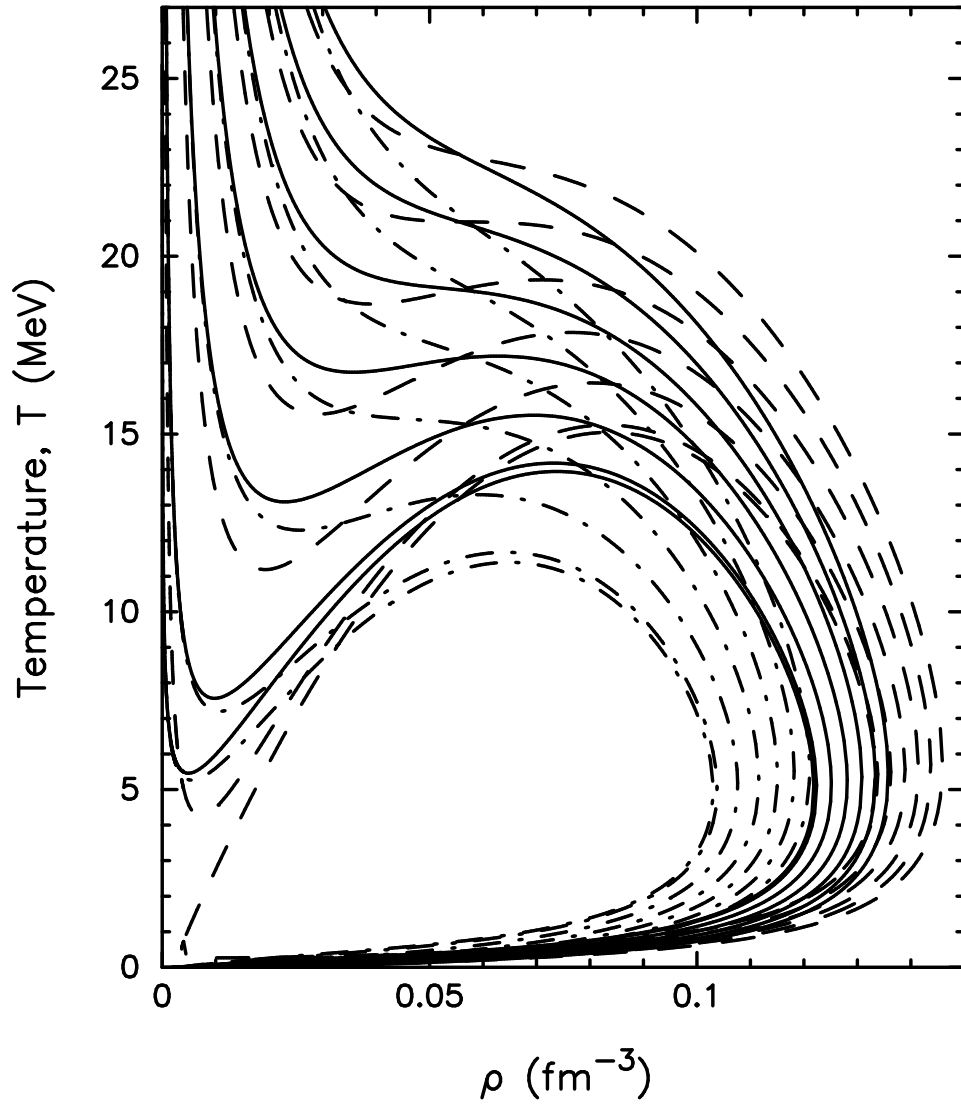


FIG. 5. Temperature $T(\rho)$ for $P = 0.0, 0.015, 0.1, 0.2, 0.3, 0.4$, and 0.5 , from bottom to top, at $y = 0.3$ (dash-dotted curve) and 0.5 (solid curve). Dashed curves are for the case without Coulomb and surface effect.

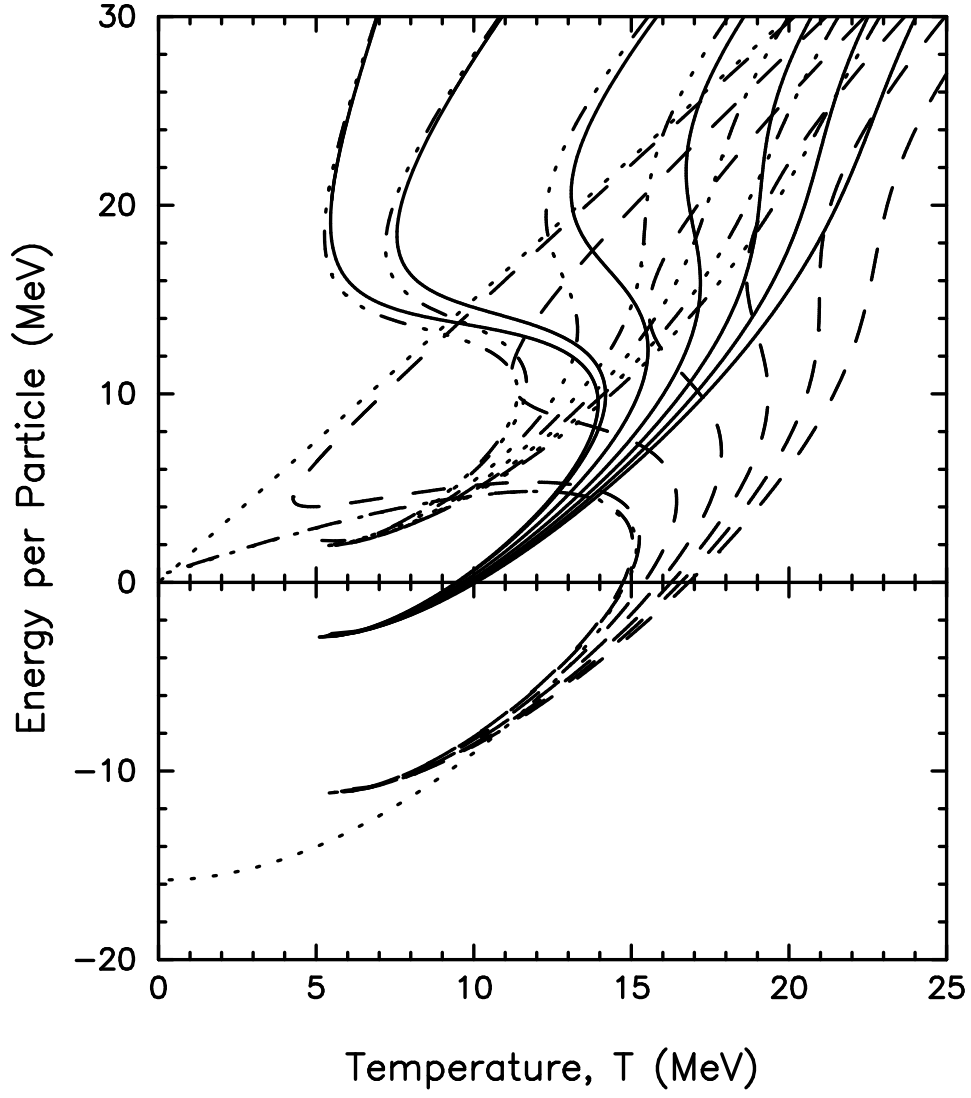


FIG. 6. Energy per particle $\mathcal{E}(T)/\rho$ for $P = 0.0, 0.015, 0.1, 0.2, 0.3, 0.4$, and 0.5 , from top to bottom, at $y = 0.3$ (dash-dot-dot-dotted) and 0.5 (solid). Dashed curves are for $y = 0.5$ without Coulomb and surface effects and dotted line is for exact result at $P = 0$ from Ref. [13]. This shows that the Fermi gas approximation we have used is not varied for T lower than about 5 MeV with high density, but very accurate for higher temperature (dashed curve for $P = 0.0$ coincide with the dotted curve for $\mathcal{E}/\rho \geq 8$ MeV).

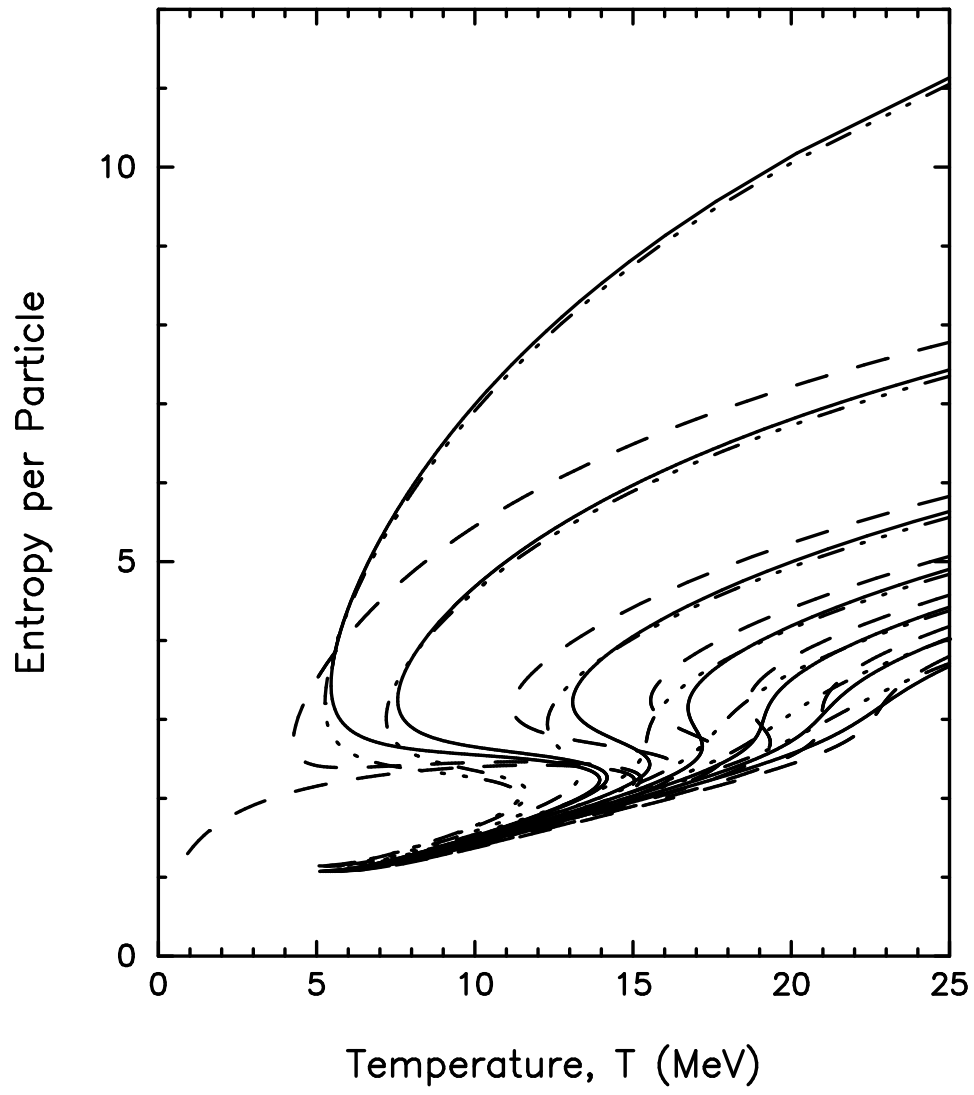


FIG. 7. Same as Fig.6 but for entropy per particle $S(T)/\rho$